LA-UR-15-26861 (Accepted Manuscript)

Cosmic Ray Muon Imaging of Spent Nuclear Fuel in Dry Storage Casks

Durham, J. Matthew; Guardincerri, Elena; Morris, Christopher; Poulson, Daniel Cris; Bacon, Jeffrey Darnell; Chichester, David; Fabritius, Joseph; Fellows, Shelby; Kurnadi, Priscilla; Plaud-Ramos, Kenie Omar; Morley, Deborah Jean; Tovey, Larry; Winston, Philip

To be published in: Journal of Nuclear Materials Management

DOI to publisher's version:

Permalink to record: http://permalink.lanl.gov/object/view?what=info:lanl-repo/lareport/LA-UR-15-26861

Cosmic Ray Muon Imaging of Spent Nuclear Fuel in Dry Storage Casks

J. Matthew Durham,[1,a] Elena Guardincerri,[1] Christopher L. Morris,[1] Daniel Poulson[1], Jeffrey D. Bacon[1], David Chichester[2], Joseph Fabritius[1], Shelby Fellows[1], Kenie Plaud-Ramos[1], Deborah Morley[1], Philip Winston[2]

[1]*Los Alamos National Laboratory, Los Alamos, NM, 87545 USA*

[2]*Idaho National Laboratory, Idaho Falls, ID 83415 USA*

Abstract: Cosmic ray muon radiography has been used to identify the absence of spent nuclear fuel bundles inside a sealed dry storage cask. The large amounts of shielding that dry storage casks use to contain radiation from the highly radioactive contents impedes typical imaging methods, but the penetrating nature of cosmic ray muons allows them to be used as an effective radiographic probe. This technique was able to successfully identify missing fuel bundles inside a sealed Westinghouse MC-10 cask. This method of fuel cask verification may prove useful for international nuclear safeguards inspectors. Muon radiography may find other safety and security or safeguards applications, such as arms control verification.

Keywords: dry cask storage, muon radiography, cosmic ray muons

I. Introduction:

The nuclear energy policy decision to suspend spent fuel reprocessing in the United States, along with the lack of a permanent repository for high-level nuclear waste, has led to the presence of ~15000 metric tons of irradiated fuel rods in above-ground dry cask storage at various sites throughout the country [1]. In other parts of the world, where spent fuel reprocessing does occur, dry casks are still in use for interim storage of irradiated fuel. This large amount of highly radioactive fuel presents a potential global security risk if any of it were diverted for illicit purposes. A continual chain of accountability and verification is a necessary safeguard.

The International Atomic Energy Agency (IAEA) typically maintains Continuity-of-Knowledge (CoK) of spent fuel through surveillance of storage sites and periodic checks of tamper-indicating devices on cask lids [2]. When independent, standalone confirmation of a dry storage casks contents is needed (either to recover from loss of CoK or to verify a member state's declaration of cask contents) the cask must be moved to a storage pool to be opened and visually inspected. This procedure is invasive, costly, time-consuming, and potentially dangerous. A non-destructive radiographic method for determining a cask's

[a] Corresponding author. Email address: *durham@lanl.gov*

contents is therefore a desirable safeguard tool. Previous studies, however, have shown that the cask's heavy shielding hinders inspection with typical radiographic techniques [3].

Cosmic ray muons offer an alternative tomographic probe. Since muons are colorless leptons, they have no hadronic interaction with nucleons, and their relatively large mass of 105.6 MeV/c^2 limits energy loss due to bremsstrahlung radiation. These properties allow energetic muons to penetrate large amounts of material that are inaccessible to other particles. Muons do possess an electric charge and undergo Coulomb scattering off nuclei as they pass through matter. Cosmic ray interactions in the upper atmosphere produce muons that arrive at the surface of the Earth at a rate of ~1/cm^2/min, with a mean energy of ~ 4 GeV [4].

The first use of cosmic ray muons for radiography was in 1955, when George measured muon attenuation to determine the overburden of rock above a tunnel [5]. This was followed by Alvarez *et al.*, who used this method to confirm the Second Pyramid of Giza did not contain any undiscovered chambers [6], and more recently by several groups examining geologic features [7] [8] [9] [10] [11]. A different method, developed at Los Alamos National Laboratory, uses measurements of the multiple scattering angle of individual muons passing through an object to create tomographic images of the object's interior structure [12]. This technique was originally developed to inspect cargo containers for illicit trafficking of nuclear material [13] [14], and has since been applied to studies of nuclear weapons, industrial corrosion [15], nuclear reactors [16] [17] [18], and is being explored as a method to determine the condition of the damaged cores of the Fukushima Daiichi nuclear power plant [19] [20]. A related technique, which uses muon-induced fission to tag fissile materials, is being explored as a technology for treaty verification [21].

While there has been considerable interest in cosmic ray muon radiography of nuclear waste in storage containers [22] [23] [24] [25] [26] [27], there have been no actual measurements made in the field to date. Here we present the first results from cosmic-ray muon radiography of spent fuel inside a partially loaded dry storage cask at Idaho National Laboratory. With this technique, we show that it is possible to determine if several fuel bundles are missing inside the sealed cask.

II Measurement:

Muons that pass through matter undergo multiple Coulomb scattering off nuclei. The angular distribution of these scattered particles can be approximated by a Gaussian of width

$$\sigma_{scat} = \frac{14.1\ \text{MeV}}{\beta c p}\sqrt{\frac{l}{X_0}},$$

where βc and p are the velocity and momentum of the incoming muon and l/X_0 is the material's thickness in radiation lengths [4] [28] [29] [30] [31]. The radiation length of a material has a strong dependence on the atomic number Z of the scattering center; for example, one radiation length of typical shielding concrete is 10.7 cm, for iron, $X_0^{Fe} = 1.76$ cm, and in uranium, $X_0^{U} = 0.32$ cm. This makes multiple scattering tomography especially sensitive to high-Z objects (i.e. uranium fuel), even if surrounded by low-Z material (concrete shielding). The scattering angles are determined by measuring the trajectories of individual muons before and after they pass through the object under inspection. Data from an ensemble of trajectories gives tomographic information on the object's internal structure. For details on image reconstruction algorithms, see [12] [14] [32].

The incoming and outgoing muon trajectories are measured with two identical drift tube tracking detectors, which are placed on opposite sides of the object under inspection. The individual tubes are made of aluminum, are 1.2 m long with an outer diameter of 5.08 cm and wall thickness of 0.89 mm, and are filled with 1 bar of a 47.5% Ar, 42.5% CF_4, 7.5% C_2H_6, 2.5% He gas mixture (see Figure 1a). A single 30 micron diameter gold-plated tungsten anode wire runs down the center of each tube. Muons passing through the tubes ionize the gas, and the resulting electrons drift towards the wire where they are multiplied through an avalanche process in the high electric field near the surface of the wire, producing a measureable signal.

The single tube efficiency as a function of anode wire voltage is shown in Fig.1b. This was measured by stacking three tubes vertically and requiring coincident hits in the top and bottom tubes, indicating that a muon had passed through the stack of three tubes. When this trigger fired, the middle tube was examined for a coincident signal. The ratio of three-level coincidences between all tubes to the number of two-level coincidences between the outer tubes gives the efficiency of the middle tube. During operation, the wire is held at a voltage of +2585 V relative to the tube wall, which gives the tubes an efficiency >90% and sufficient gain to satisfy signal thresholds in the readout electronics.

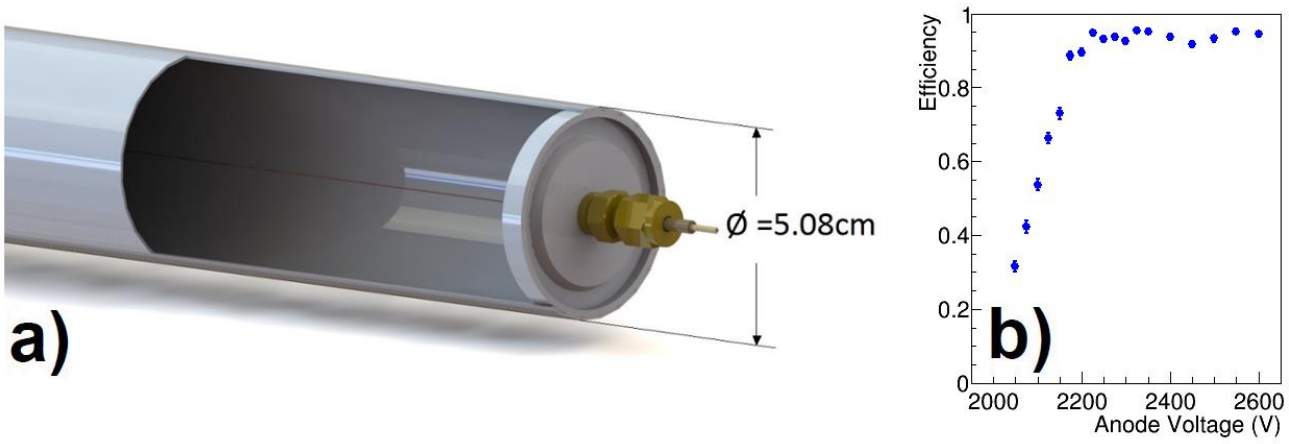

Figure 1: Cutaway drawing of a single drift tube detector, showing the anode wire inside the 5.08 cm OD tube (a). The muon detection efficiency of a single tube as a function of anode wire voltage (b).

Each individual drift tube measures the radial distance from the wire where the muons passed with an accuracy of ~few hundred microns. The inherent left/right ambiguity in single tubes is resolved by using double layers of tubes, which are offset in the radial direction by a distance equal to one tube radius. Stacks of six double layers, arranged with orientations alternating by 90 degrees in order to provide sensitivity in two coordinates, form a complete tracker (see Figure 2). Muon tracks are reconstructed by fitting patterns of hits in the tube layers.

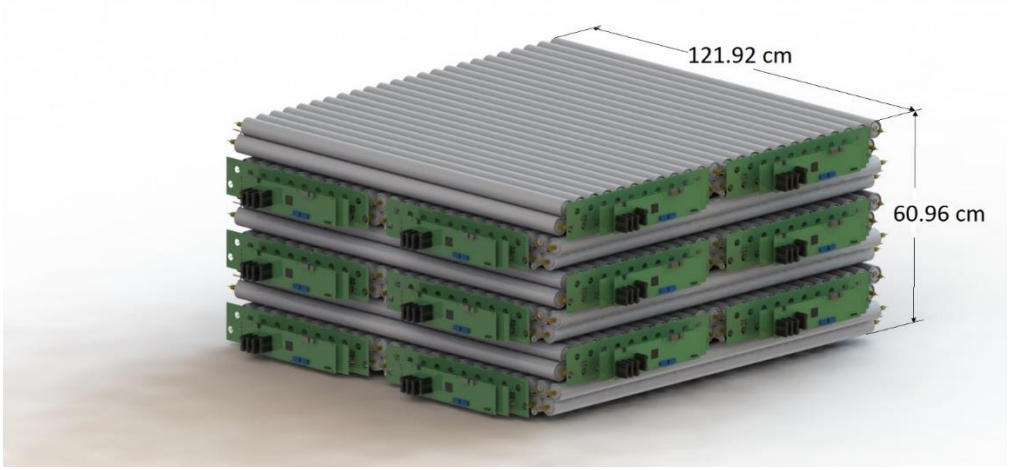

Figure 2: A drawing of one muon tracker, consisting of 288 individual drift tubes with read out electronics. Multiple layers of tubes in alternating orientations allow multi-dimensional particle tracking. Support structures are not shown for clarity.

The object under inspection for this measurement was a partially loaded Westinghouse MC-10 spent fuel cask located at the Idaho National Laboratory [33]. The MC-10 is a vertical storage cask that is 4.8 m high and 2.7 m in diameter. The cask has a basket for 24 pressurized water reactor fuel assemblies inside a 25 cm thick forged steel cylindrical container that is surrounded by a layer of BISCO NS-3 neutron

shielding and an outer stainless steel skin. Two identical muon tracking detectors were placed on opposite sides of the cask in order to record the incoming and outgoing tracks of muons which traverse the cask. Since the cosmic ray muon flux is approximately proportional to $\cos^2\theta_z$, where θ_z is the angle from the zenith, one detector was elevated by 1.2 m relative to the other to increase muon counting rates. A larger elevation of the upper detector would decrease the sampled zenith angle and therefore increase the muon flux through both detectors; however, considerations of the ease of setup and stability of the detector on the stand limited the allowed height. The instruments were placed in thin-walled weatherproof enclosures to protect them from precipitation during the measurement. Figure 3 shows a photograph of the setup around the MC-10 cask.

Figure 3: Muon tracking detectors in weatherproof enclosures around the MC-10 cask at Idaho National Lab. One detector is elevated relative to the other, to take advantage of the higher muon flux at smaller zenith angles.

Despite the heavy shielding, there is still a significant radiation field outside the MC-10 cask which can potentially interfere with muon tracking. Measurements showed ~0.1 mSv/h (10 mrem/h) of neutrons and ~0.1 mSv/h of gamma ray activity on contact with the cask surface. Compton scattered electrons can produce spurious hits in single drift tubes, which can affect the track reconstruction algorithms. To remove this background, a trigger was added in the data acquisition system that required hits in neighboring tubes within a time window of 600 ns in order to be considered as part of a track candidate. In standalone tests

away from the cask, it was found that inefficiencies in this trigger requirement reduced track counting rates by ~50%. During the measurement, cosmic ray tracks that went through both detectors and the cask were recorded at a rate of ~0.25 Hz. Data was collected around the MC-10 cask for ~200 hours, recording 1.62×10^5 muon tracks that passed through the cask and both detectors.

The loading profile of the MC-10 cask is shown in Figure 4, relative to the muon tracking detector placement. The detectors are not large enough to image the entire cask body, so they were positioned such that the field of view covered the columns of most interest, which contain one, six, five, and four intact spent fuel bundles. The bundles that are present in the cask are Westinghouse 15 x 15 pressurized water reactor fuel, with nominal burn up of 30,000 MWd. Each of the bundles are 21 cm on each side with a total height of 4.06 m, of which the fuel column is 3.66 m. Twenty of the 225 possible rod locations in each assembly are occupied by guide tubes for control rods, and the centermost spot is used for in-core instrumentation. The remaining 204 slots are filled with 1.07 cm diameter fuel rods. These assemblies were removed from a US commercial power reactor in the early 1980s.

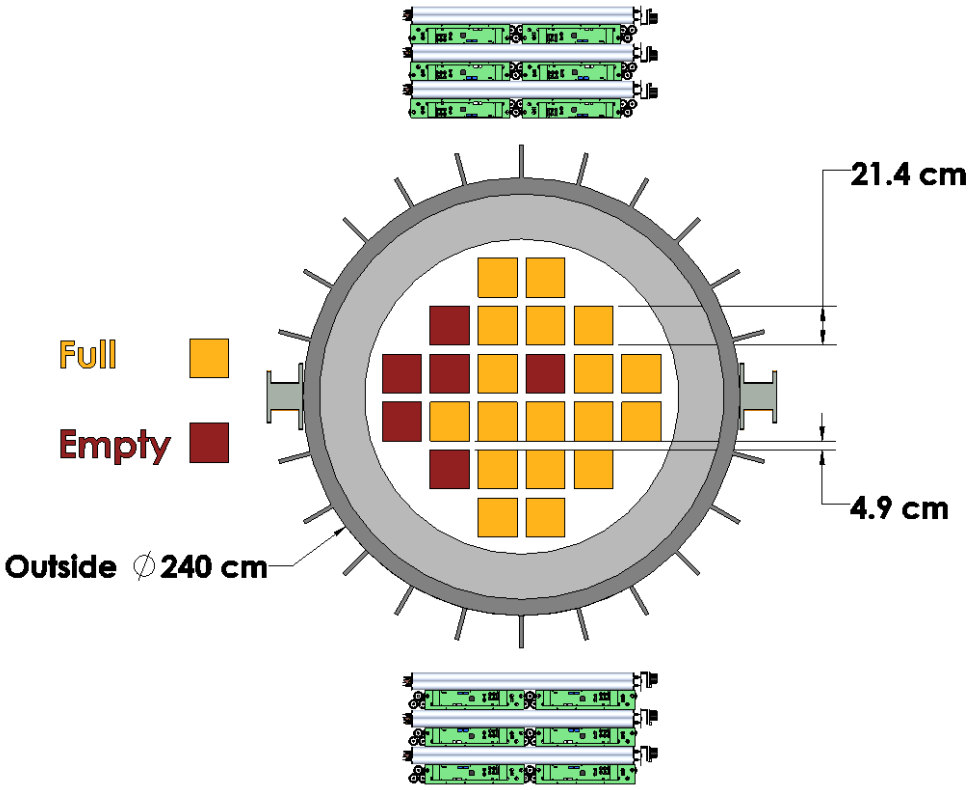

Figure 4: Top-down view of the loading profile of the MC-10 cask at Idaho National Laboratory. Approximate locations of the two muon tracking detectors are shown for comparison.

III. Results and Discussion:

The measured muon trajectories are projected to a plane parallel to the detectors positioned near the center of the cask. This plane is divided into 2 cm x 2 cm voxels. Each voxel has a corresponding histogram, where the scattering angles of each track that pass through that voxel are collected. From the expression previously given for σ_{scat} we see that the scattering angles are highly dependent on the muon's momentum. The scattering histograms are fit with amplitudes corresponding to seven different groups of muon momentum, which provides a more realistic representation of the cosmic ray muon energy spectrum (see [32] for details). A typical scattering angle histogram is shown in Figure 5. The radiation length weighted areal density l/X_0, which is closely related to the thickness in units of radiation length traversed by muons which pass through that voxel, is extracted from the fit information.

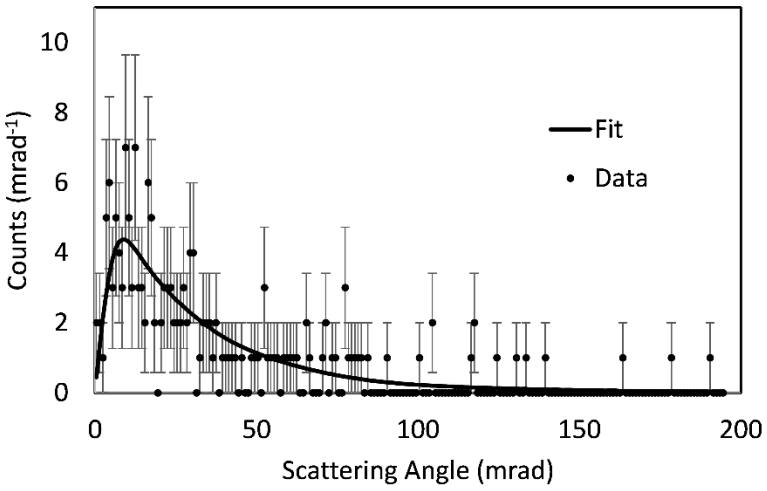

Figure 5: A typical scattering angle histogram, along with the multigroup fit. These histograms are stored for each voxel and are used to determine the areal density traversed by muons that pass through the cask.

An image of the cask in terms of the areal density extracted from each voxel is shown in Figure 6a. From left to right, the columns within the muon tracker's field of view contain one, six, five, and four assemblies

(see Figure 4). It is apparent that the column with only one fuel assembly has significantly less areal density than the neighboring column with six assemblies.

For comparison, Monte Carlo simulations were performed with GEANT4 [34], for three different spent fuel loading configurations, and the areal density image was obtained using identical analysis techniques. Figure 6b shows the image obtained with 10 million simulated muon trajectories through the MC-10 cask with the same partial defect in loading as the measurement. Figures 6c and 6d show the image that would be obtained for fully-loaded and empty casks, respectively.

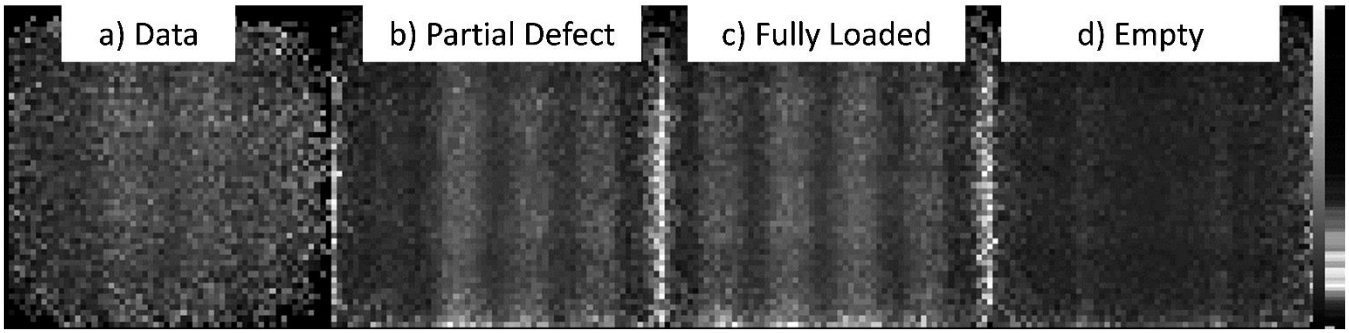

Figure 6: Image of the cask in terms of areal density, for the measured MC-10 cask (a) and GEANT4 simulations of three different loading configurations (b-d).

The individual fuel assemblies contained in the cask are near uniform in the vertical direction. The cask body is also uniform in this direction over the field of view of this measurement. Therefore, the areal densities shown in Figure 6 are not expected to vary with height. Recognizing this, the two-dimensional areal density data are projected (summed over the voxel data) onto the horizontal axis and shown in Figure 7. This vertically integrated areal density metric is sensitive to the total amount of material along the path the muons take between the two detectors.

A clear difference is seen between the columns with different loading profiles. The column with only one fuel assembly on the left edge of the field of view shows a significantly smaller areal density than all the other columns. As expected, the fully loaded column with six fuel assemblies shows the greatest areal density, and is clearly distinguishable from the columns with one and four fuel bundles. The statistical uncertainties on the data prevent a definitive statement from being made about the column with five assemblies; however, the simulations show that higher statistics measurements will be able to effectively identify that defect.

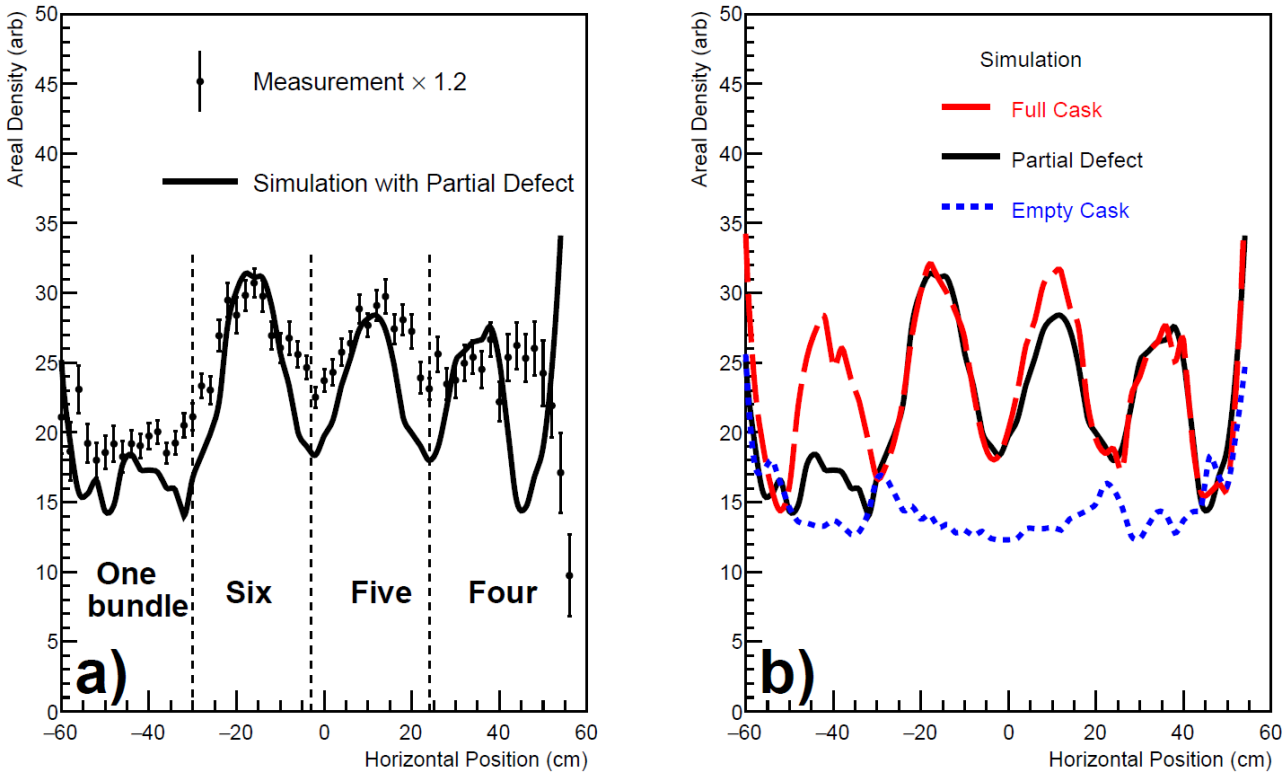

Figure 7: The measured areal density through the cask (a), compared to a GEANT4 simulation of a cask with the same partial defect in loading. Dashed lines show the approximate boundaries of columns in the fuel basket. Simulations of a completely full and empty cask are shown in panel (b) for comparison.

The simulated model of the fully loaded cask shows the expected variation across the view of the fuel basket, with the columns containing four fuel bundles on the edges and two fuel bundles in the center. The partially loaded cask shows clear variation, with similar structure to the measurement. The data shown in Figure 7 was scaled by a factor of 1.2 to more closely resemble the scale of the simulation. This is likely due to differences in the muon momentum spectrum used in the simulation and the actual muon momentum that is present in nature at the measurement site. There is little existing data on the muon momentum spectrum at large zenith angles and momenta less than 10 GeV/*c* that can be used to constrain models of cosmic ray muon distributions in this region, so in this regard the simulation may not accurately depict reality. Near the edge of the field of view, the detector acceptance is limited and biased towards tracks which cross long path lengths through the cask, resulting in unphysically large areal densities within ~5cm of the edges of the field of view. However, no conclusions are drawn from the data affected by these artifacts.

We also note that a precise alignment of the muon tracking detectors with the fuel columns in the cask was not performed. There may be offsets of ~several cm between the center of the detector and the center of the cask, as well as misalignment between the plane in between the detectors and the fuel columns. These misalignments can introduce aberrations in the reconstructed images and areal densities that contribute to differences between the data and simulation. A more precise alignment will be performed in future measurements.

IV. Summary and Outlook:

We have shown that cosmic ray muon scattering angles can be used to infer the areal density of loaded dry storage casks, and thereby determine if fuel assemblies are present or missing in certain configurations. The data shown was collected over a period of ~200 hours on a partially loaded MC-10 cask at Idaho National Laboratory. This technique may be a useful tool for maintaining CoK of spent fuel in dry cask storage.

Simulations show that measurements with better statistical precision will be able to more effectively discriminate between fully loaded and partially loaded fuel columns, and may be able to determine if portions of individual fuel bundles are missing, however, additional studies are needed to determine absolute sensitivities of the technique to partial defects in individual fuel bundles. In addition, a more precise alignment of the muon tracking detectors and the fuel columns will reduce aberrations in the reconstructed images. The density analysis performed here is integrated through the cask in the direction between the two muon tracking detectors, and therefore can locate columns where assemblies are missing, but does not measure the depth within the cask. If additional data is taken with the detectors rotated around the cask, the position ambiguities could be resolved and missing assemblies could be located in three dimensions. Future measurements to collect additional data from several viewing angles with a more careful alignment are currently being planned.

We note here that the two planar muon trackers used for this measurement are not optimized for measurements of relatively large cylindrical objects. A muon tracking detector could be designed such that it surrounds cask completely and simultaneously measures muons coming from all azimuthal angles, giving a complete tomography of the cask's interior. Increasing muon detector coverage and decreasing

the sampled zenith angle would also decrease the counting time necessary for statistically significant results. Designs and analysis of such an optimized instrument that could be fielded by international safeguards inspectors are currently underway.

V. Acknowledgements:

This work is funded by the National Nuclear Security Administration's Office of Defense Nuclear Nonproliferation Research & Development. We thank P. Kurnadi and L. Tovey of Decision Sciences International Corporation and W. Schwendiman of INTEC for valuable assistance. This document is released under LA-UR-15-26861.

References

[1] L. H. Hamilton, B. Scowcroft, et al., "Blue Ribbon Commission on America's Nuclear Future Report to the Secretary of Energy," 2012.

[2] G. Zuccaro-Labellarte and R. Fagerholm, "Safeguards at Research Reactors, Current Practices, Future Directions," *IAEA Bulletin, vol. 38, no 4,* 1996.

[3] K. P. Ziock et al., "Radiation Imaging of Dry-Storage Casks for Spent Nuclear Fuel," *Nuclear Science Symposium Conference Record, 2005 IEEE,* pp. 1163-1167, 2005.

[4] K. A. Olive et al. (Particle Data Group), "The Review of Particle Physics," *Chinese Physics C,* vol. 38, no. 090001, 2014.

[5] E. P. George, "Cosmic Rays Measure Overburden of Tunnel," *Commonwealth Engineer,* pp. 455-457, 1955.

[6] L. W. Alvarez et al., "Search for Hidden Chambers in the Pyramids," *Science,* vol. 167, pp. 832-839, 1970.

[7] K. Nagamine, M. Iwasaki, K. Shimomura, K. Ishida, "Method of probing inner-structure of geophysical substance with the horizontal cosmic-ray muons and possible application to volcanic eruption prediction," *Nuclear Instruments and Methods A,* vol. 356, no. 2, pp. 585-595, 1995.

[8] N. Lesparre et al., "Geophysical muon imaging: feasibility and limits," *Geophysical Journal International,* vol. 183, pp. 1348-1361, 2010.

[9] L. Olah et al., "Cosmic Muon Detection for Geophysical Applications," *Advances in High Energy Physics,* vol. 2013 Article ID 560192, 2013.

[10] C. Carloganu et al. (TOMUVOL Collaboration), "Towards a Muon Radiography of the Puy de Dome," *Geoscientific Methods, Instrumentation and Data Systems,* vol. 2, no. 1, pp. 55-60, 2013.

[11] F. Ambrosino et al., "The MU-RAY project: detector technology and first data from Mt. Vesuvius," *Journal of Instrumentation,* vol. 9, 2014.

[12] L. Schultz et al., "Image reconstruction and material Z discrimination via cosmic ray muon radiography," *Nuclear Instruments and Methods A,* vol. 519, no. 3, pp. 687-694, 2004.

[13] K. Borozdin et al, "Surveillance: Radiographic imaging with cosmic-ray muons," *Nature,* vol. 422, no. 277, 2003.

[14] W. Priedhorsky et al., "Detection of high-Z objects using multiple scattering of cosmic ray muons," *Revue of Scientific Instruments,* vol. 74, no. 10 , 2003.

[15] J. M. Durham et al., "Tests of cosmic ray radiography for power industry applications," *AIP Advances,* vol. 5 067111, 2015.

[16] T. Sugita et al, "Cosmic-ray muon radiography of UO2 fuel assembly," *Journal of Nuclear Science and Technology,* vol. 51, no. 7-8, pp. 1024-1031, 2014.

[17] C. L. Morris et al, "Analysis of muon radiography of the Toshiba nuclear critical assembly reactor," *Applied Physics Letters,* Vols. 104, 024110, 2014.

[18] J. O. Perry et al., "Imaging a nuclear reactor using cosmic ray muons," *Journal of Applied Physics,* Vols. 113, 184909, 2013.

[19] K. Borozdin et al., "Cosmic Ray Radiography of the Damaged Cores of the Fukushima Reactors," *Physical Review Letters,* Vols. 109, 152501, 2012.

[20] H. Miyadera et al., "Imaging Fukushima Daiichi reactors with muon," *AIP Advances,* Vols. 3, 052133, 2013.

[21] E. Guardincerri et al., "Detecting special nuclear material using muon-induced neutron emission," *Nuclear Instruments and Methods A,* vol. 789, pp. 109-113, 2015.

[22] J. Gustafsson, *Tomography of Canisters for Spent Nuclear Fuel Using Cosmic-ray Muons,* Uppsala, Sweden: Thesis, Uppsala University, 2005.

[23] M. Osterland et al., "Tomography of Canisters for Spent Nuclear Fuel," in *Proceedings of the International Workshop on Fast Neutron Detectors and Applications*, Cape Town, South Africa, 2006.

[24] G. Jonkmans et al., "Nuclear waste imaging and spent fuel verification by muon tomography," *Annals of Nuclear Energy,* vol. 53, pp. 267-273, 2013.

[25] F. Ambrosino et al., "Assessing the feasibility of interrogating nuclear waste storage silos using cosmic-ray muons," *Journal of Instrumentation,* vol. 10 T06005, 2015.

[26] A. Clarkson et al., "The design and performance of a scintillating-fibre tracker for the cosmic-ray muon tomography of legacy nuclear waste containers," *Nuclear Instruments and Methods A,* vol. 745, pp. 138-149, 2014.

[27] S. Chatzidakis et al., "Monte Carlo Simulations of Cosmic Ray Muons for Dry Cask Monitoring," *Transactions of the American Nuclear Society,* vol. 112, no. 1, pp. 534-536, 2015.

[28] G. Moliere, "Theory of the scattering of fast charged particles," *Zeitschrift fur Naturforschung,* vol. 3a, p. 78, 1948.

[29] H. A. Bethe, "Moliere's Theory of Multiple Scattering," *Physical Review,* vol. 89, p. 1256, 1953.

[30] V. L. Highland, "Some practical remarks on multiple scattering," *Nuclear Instruments and Methods,* vol. 192, no. 2, p. 497, 1975.

[31] G. R. Lynch and O. I. Dahl, "Approximations to multiple Coulomb scattering," *Nuclear Instruments and Methods B,* vol. 58, no. 1, p. 6, 1991.

[32] J. O. Perry et al., "Analysis of the multigroup model for muon tomography," *Journal of Applied Physics,* Vols. 115, 064904, 2014.

[33] M. A. McKinnon et al., "The MC-10 PWR Spent-Fuel Storage Cask: Testing and Analysis," Electric Power Research Institute Report NP-5268, 1987.

[34] S. Agostinelli et al., "GEANT4 - a simulation toolkit," *Nuclear Instruments and Methods in Physics Research Section A,* vol. 506, no. 3, pp. 250-303, 2003.